Bipolar photodiode module operated at 4 K

[1]Bardalen, Eivind; [2]Nissilä, Jaani; [2]Fordell, Thomas; [3]Karlsen, Bjørnar; [4]Kieler, Oliver; [1]Øhlckers, Per

[1]Department of Microsystems - University of South-Eastern Norway
[2]VTT MIKES - Finland
[3]Justervesenet - Norway
[4]Department 2.4 Quantum Electronics - Physikalisch-Technische Bundesanstalt, Germany

Bardalen, E., Nissilä, J., Fordell, T., Karlsen, B., Kieler, O., & Ohlckers, P. (2020). Bipolar photodiode module operated at 4 K. In 2020 IEEE 8th Electronics System-Integration Technology Conference (ESTC). https://doi.org/10.1109/ESTC48849.2020.9229695

Publisher's version: DOI: 10.1109/ESTC48849.2020.9229695

Bipolar photodiode module operated at 4 K

Eivind Bardalen
Department of Microsystems
University of South-Eastern Norway
Norway
eba@usn.no

Jaani Nissilä
VTT MIKES
Espoo, Finland

Thomas Fordell
VTT MIKES
Espoo, Finland

Bjørnar Karlsen
Justervesenet
Kjeller, Norway

Oliver Kieler
Department 2.4 Quantum Electronics
Physikalisch-Technische Bundesanstalt
Braunschweig, Germany

Per Ohlckers
Department of Microsystems
University of South-Eastern Norway
Norway

***Abstract*—An optoelectronic module for generating high frequency bipolar current pulses at 4 K was developed. Bipolar signals are generated by connecting a pair of photodiodes in series to coplanar waveguides on silicon. The transmission line pulse propagation was simulated in COMSOL. A planar optical fiber connector was fabricated, where the end fiber faces where angle polished to reflect the beam perpendicular to the fiber. An assembled prototype was fabricated by flip-chip bonding photodiodes to the silicon photodiode carrier. The optical connector was aligned and bonded using epoxy. The prototype was tested using a mode-locked laser producing pulses with sub-20 ps pulses. Bipolar output pulses were generated at 4 K and measured using an oscilloscope. The measured output pulses were affected by ringing and were broader than the reference signal. Comparison with simulations indicate that the ringing was caused by reflections at wirebonds.**

Keywords— Optoelectronics, flip-chip bonding, packaging, photodiodes, RF simulation, voltage metrology, cryogenics, RF measurements.

I. Introduction

In voltage metrology, for many years, systems based on Josephson junctions have become the standard for generating quantum accurate voltages. The Josephson Arbitrary Waveform Synthesizer (JAWS) is pulse-drive variant, operated by passing short current pulses through Josephson junction arrays (JJA). When operated at cryogenic temperatures, typically around 4 K, the voltage across the JJA follows the formula:

$$V = n \cdot N \cdot \Phi_0 \cdot f \qquad (1)$$

where n the quantum step number, N is the number of junctions, $\Phi_0 = h/2e$ is the flux quanta and f is the pulse bit rate. Hence, by encoding a desired waveform in the pulse train, a time-dependent voltage can by synthesized. To date, these kinds of systems have been demonstrated with output voltages up to and above 1 V_{RMS} [1-4].

A major challenge in operating these systems is due to the fact that the low T_c Nb-based Josephson junctions must be operated at cryogenic temperatures, typically at 4 K by immersion in liquid helium. Conventionally, JAWS have been operated with high-frequency coaxial electrical cables connecting the room-temperature pulse pattern generator and the JAWS chip. The typical length of the cryoprobe is about 1 m. Recently, there has been substantial effort put towards developing an optically controlled pulse-drive, replacing the coaxial cables with optical fibers coupled to photodiodes (PD) at the cold end close to the JAWS chip.

This kind of setup increases the complexity of the system, as a number of additional components are required, including laser sources, optical modulators and fiber optic components. However, several advantages are also expected, as optical fibers are capable of transmitting very high frequencies with low loss and low electromagnetic interference. Additionally, using optical links electrically decouples the JJA from the room temperature operated high frequency sources, thereby eliminating coupling noise, especially at higher frequencies in the MHz range. By splitting the optical signal, it is possible to easily control several JAWS arrays in parallel to increase the output voltage. The reduction of room temperature pulse-channels will decrease the overall costs of such a JAWS system too, which might help to commercialize the system.

In the EMPIR projects Q-WAVE and QuADC, the use of cryogenically operated PDs were demonstrated [5-9]. In these projects, InGaAs PDs were flip-chip bonded to silicon substrates and optical fibers were connected by use of epoxy bonded glass alignment sleeves. These assemblies proved to be reliable and were capable of transmitting high-frequency pulses with a data rate up to 30 Gbit/s. However, they were only designed to transmit unipolar pulses, unlike electrical cables, which may transmit bipolar signals. Using bipolar pulses will double the output voltage of a JAWS chip with a given number of junctions, because both the positive and negative Shapiro steps are addressed. This is a very important feature of a JAWS system for many applications.

In order to generate bipolar voltages from a single JAWS chip, a pair of PDs is needed, with the output terminals of each PD connected in reverse with respect to the other PD.

There are several technical difficulties associated with this approach, including the fiber-optical connection to the closely spaced pair of PDs, as well as the design of the coplanar waveguide (CPW) transmission lines. In addition, the electro-optical pulse generation system for effectively controlling the optical input to each PD must be designed.

Here, we describe work done on fabricating the cold part of the system, meaning the fiber-coupled PDs and transmission lines.

II. RF Design and Simulations

A. RF Design

The bipolar PD module converts a high-frequency optical input from an optical fiber to electrical pulses using two high-

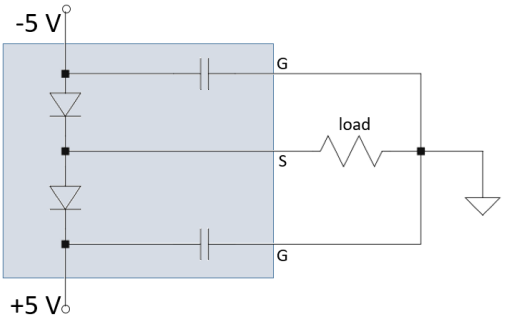

Fig. 1. PD module circuit. Components inside the grey area are on the Si carrier, while external connections are outside. On-chip capacitors allow the high-frequency pulses to pass, while blocking the DC current from the bias voltage source.

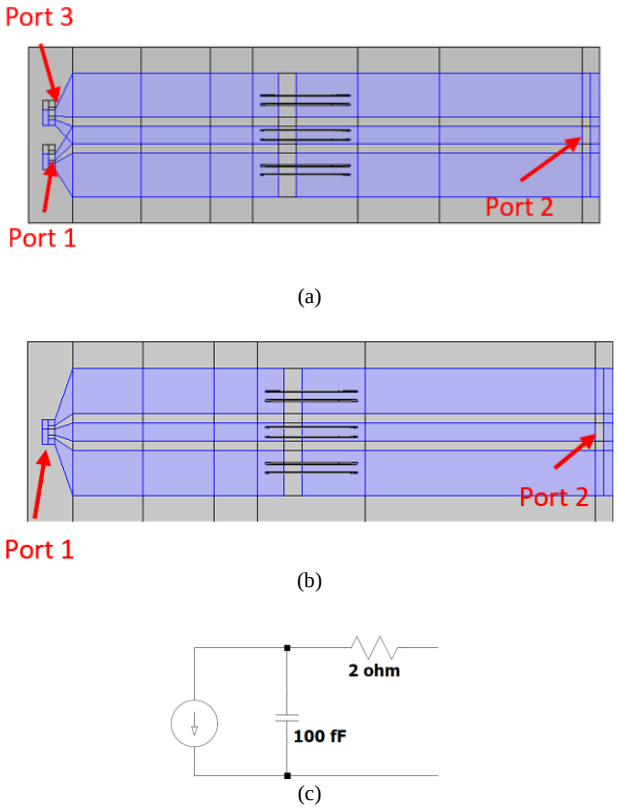

Fig. 2. COMSOL model of the electrical transmission lines on the Si PD bipolar (a) unipolar (b) carriers and connection to PCBs. 25 µm wire bonds with 1 mm length are modelled as connection between the PD carrier and PCB. (c): Equivalent lumped circuit used to model ports 1 and 3.

speed Albis PD20X1 lensed InGaAs PDs. The PDs are connected to a silicon chip carrier having superconducting Nb transmission lines and bias connections. The chip carrier is mounted to a printed circuit board (PCB) terminated by SMA connectors for external measurements.

The electrical output from each pair of PDs is connected to a CPW, which are compatible with the JAWS chips. Since the CPW has a G-S-G (ground-signal-ground) configuration, the PD pair share the center conducting line and is connected in series, as illustrated in Fig. 1.

This configuration necessarily reduces the performance compared the single connected PDs. This performance reduction is due to several factors:

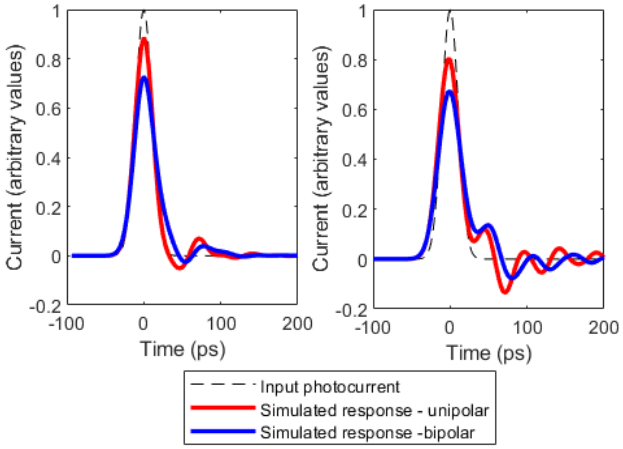

Fig. 3. Simulated response to a Gaussian input signal with 25 ps full width of half maximum (FWHM). Left: Response for continuous CPW. Right: Response for CPW linked by wire bonds.

- Since each PD in practice is only directly connected to two of the conductor planes, the electrical pulse experiences a different characteristic impedance than a G-S-G connected PD.
- As the bandwidth of PDs is largely determined by its capacitance, the two series-connected PDs doubles the effective capacitance, causing a reduction of the bandwidth by a factor of two.
- The physical spacing between the PDs leads to a merging point, generating unwanted reflections.

An early prototype was based on previous designs for unipolar modules and fiber-coupling structures. In these designs, the optical fibers were separately connected to each PD by the use of glass alignment sleeves, requiring a large distance between individual fibers. Tests of this prototype ("QuADC3") showed large ringing effects in the output when illuminated with short (< 50 ps) optical pulses [10]

Based on these results, improved chip carrier prototypes ("QuADC4") were developed, providing a fundamental reduction of spacing the PDs only 500 µm apart, only slightly larger than the geometrical dimensions of the PD, which is 350 µm x 350 µm.

The time-dependent pulse propagation was simulated in COMSOL Multiphysics, using the RF module. The QuADC4 bipolar transmission lines were modelled as perfect electric conductors on silicon, as shown in Fig. 2 (a). For comparison, a unipolar configuration was also modelled, as shown in Fig. 2 (b). The photodiodes were modelled using lumped port inputs, using a simple PD model, as shown in Fig. 2 (c), with the input signal modelled as a current source. The output signal was detected at port 2, assuming 50 Ω output impedance, corresponding to the JAWS array input impedance and the typical characteristic impedance for coaxial cables. The transition between the Si carrier and PCB were modelled both as a gap between the transmission lines connected by wire bonds with 1 mm length, and for comparison, as a continuous CPW.

Fig. 3 shows the simulated response for both models for a Gaussian input pulse with full width at half maximum (FWHM) of 25 ps. It can be seen that for the bipolar PD carrier, the peak current is reduced slightly compared to the unipolar carrier. In addition, the pulse width is larger. It can

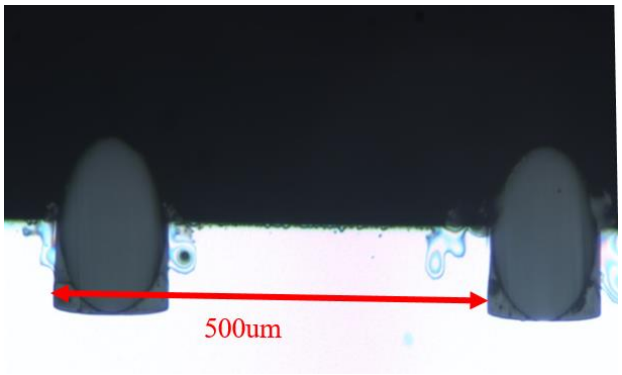

Fig. 4 Microscope image of the angle polished Si connector/optical fiber endface.

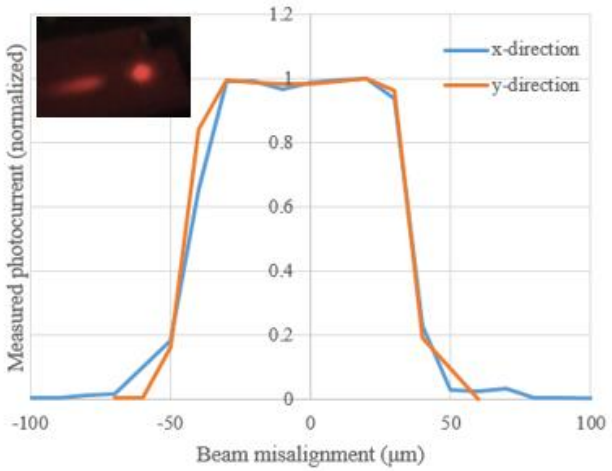

Fig. 5 Measured photocurrent against misalignment in two direction (x-direction: along fiber length, y-direction: perpendicular to fiber length). Photo inset shows the beam profile as seen on photosensitive laser viewing card.

be seen that introducing wire bonds leads to significant ringing as the electromagnetic pulse is reflected at the interface.

III. Optical Design and Assembly

The needed small 500 μm spacing of the PDs required a custom technique for coupling the fiber pairs to the PD. A planar type connector was desired, as it reduces the space needed compared to perpendicularly attached fibers. As the PDs are illuminated through a top side lens, the beam must be reflected 90º from the optical fiber. By using the principle of internal reflection, the reflective side can be made by polishing the fiber end at 45º. Theoretically, this leads to total internal reflection (TIR) at incidence angles larger than

$$\theta_c = \arcsin\left(\frac{n_2}{n_1}\right),$$

where n_1, n_2 are the refractive indices of the optical fiber and the atmosphere, respectively. For SMF-28 optical fibers, $n_2 \approx 1.47$, leading to $\theta_c \approx 42.9°$ in air ($n_1 = 1.000$). However, as the module is to be operated in liquid helium, having $n_1 = 1.0257$ [11] the critical angle increases to 44.2º. To accommodate for this change, the fiber was polished at an angle slightly larger than 45º.

Silicon substrates were patterned by photolithography and etched using deep reactive ion etching (DRIE) in order to make 60 um deep grooves with 127 μm width for the fiber pairs. SMF-28 optical fiber with 900 μm jacket were used, with 1 cm of the fiber stripped to the 125 μm cladding. The stripped part of the fibers were then placed into the grooves and Stycast 1266 epoxy was applied to one side. Due to the low viscosity of the epoxy, the groove was filled with epoxy due to capillary force. The fiber end faces were polished at 45º by fixing the silicon connectors in a 3D printed holder. A polishing process started with rough polishing with sand paper in a grinding machine, followed by polishing in 3 μm and 1 μm diamond suspension. The final polished fiber end faces of a fiber pair is shown in Fig. 4.

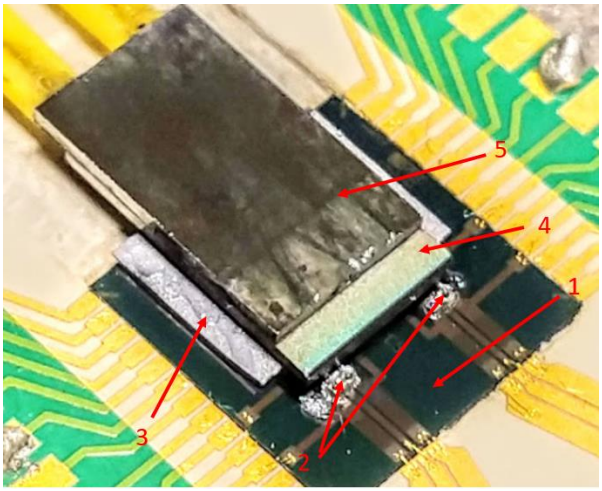

Fig. 6 Assembled prototype ("QuADC4") containing two bipolar channels outputs.. Photodiodes (2) are bonded to the silicon chip carrier (1). The optical fiber connector (4) is aligned and bonded to the photodiodes separated from the chip carrier with a spacer (3). An additional silicon block is bonded to the backside of the optical connector in order to provide support for the optical fibers.

The resulting beam profile was investigated by measuring the photocurrent from an Albis PD20X1 PD, sweeping the output beam across the PD in two directions at room temperature. A 1310 nm laser source was used as the input. As seen in Fig. 5, the photocurrent is stable against misalignments up to ± 40 μm and decreases rapidly for higher misalignments. As the photocurrent has a lens diameter of 100 μm, this indicates that the beam output is nearly circular. Hence, the roughness of the polished fiber face is sufficiently low, such that reflection was largely specular. However, a weaker second spot, due to a refracted beam, is also visible in Fig. 5. Thus, internal reflection was not total, possibly due to roughness of the polished fiber face.

Fig. 6 shows the assembled prototype. The PDs were bonded to the Si carrier using a thin layer of AuSn solder deposited directly on the PD pads by the manufacturer. After bonding, the photodiodes were underfilled with Stycast 1266 epoxy, as described in [6]. The Si substrate was adhesively bonded to the PCB, which consisted of a Ro3006/FR2 PCB with CPW transmission lines terminated by a SMA connector. Wire bond connections were made between the Si carrier and PCB, providing connections to bias and signal lines.

A 300 μm thick Si spacer was adhesively bonded to the Si carrier in order to compensate for the approximately 200 μm height of the photodiodes. The PCB assembly was then fixed to a 3-axis micrometer stage while the optical connector was fastened above the PCB assembly. The two parts were then aligned by monitoring the photocurrent from a pair of PDs. When maximum photocurrent was reached, the PCB

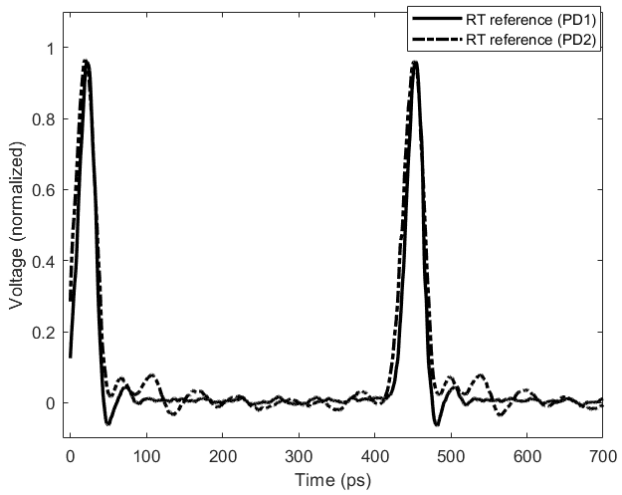

Fig. 9. Reference measurement of optical pulses at room temperature (RT) using commercially packaged PD modules. Voltage is measured over the oscilloscope 50 Ω termination.

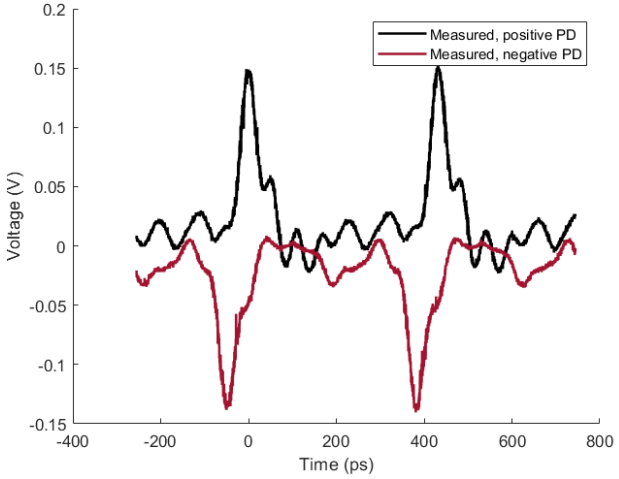

Fig. 7. Measured PD response of sample at 4 K. Voltage is measured over the oscilloscope 50 Ω termination. Graphs were adjusted in x-direction for comparison.

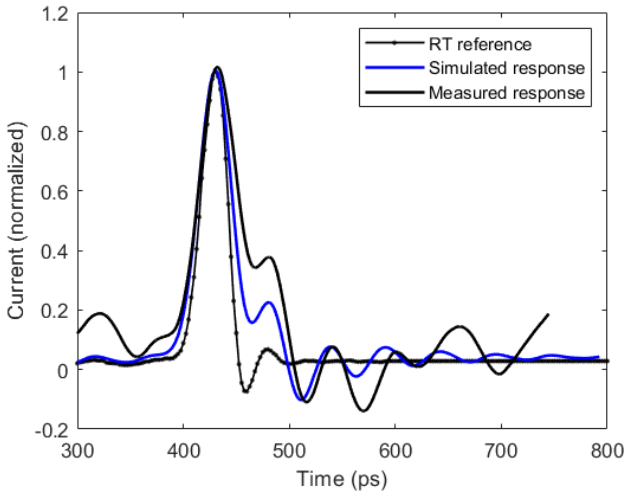

Fig. 8. Comparison of measured PD module output with simulated results.

assembly was brought into contact with the optical connector and glued permanently in place using epoxy.

IV. Measurements at Low Temperatures

Measurements of the PD response to short optical pulses were performed at VTT MIKES. A hybrid-mode-locked laser at 1340nm producing sub-20ps pulses was used [12]. The measurements were performed with an Agilent 86112A (20 GHz) sampling module in a 86100A oscilloscope frame. First, reference measurements were carried out to identify effects arising from the cryoprobe coaxial connections between the PD and the oscilloscope. Two commercial Albis PD modules were used (PD1 and PD2). PD1 acts in all measurements as a monitor of the pulsed laser performance and is connected directly to the oscilloscope input, while PD2 is connected to the oscilloscope through the whole chain of coaxial elements present also in the 4 K measurements. The coaxial components were at room temperature in these measurements. Fig. 9 illustrates the influence of the coaxial connections of the cryoprobe. As seen, the data from PD2 show some more ringing compared to PD1. PD1 has a FWHM of around 24 ps while PD2 has a FWMH of around 30 ps.

Fig. 7 shows the response of each PD in the QuADC4 sample at 4 K in terms of voltage over the 50 Ω termination. The pulse shape from each PD was similar and opposite to each other. The PD output peak voltages were slightly different, and can be attributed to variations in the optical coupling efficiency. However, the measured signal was heavily influenced by ringing compared to the reference signals. Both PDs gave peak voltages of around 0.15 V, corresponding to 3 mA. The output pulses have a FWHM of around 42 ps, significantly longer than the reference signal.

To compare the measured results with simulations, the reference input signal in (PD1) was used as input in the COMSOL model. As shown in Fig. 8, the resulting simulated pulse shape of the positive PD resembles the measured pulse, however with less pronounced ringing. In addition, the measured pulse is significantly wider than the simulated pulse.

V. Discussion

We have demonstrated the feasibility of a compact optical module for driving JAWS circuits with bipolar input. The module survived cooling to 4 K and was able to produce distinct bipolar current pulses. However, the pulses were significantly distorted compared to a reference signal and simulation results. While some of the ringing and pulse broadening may be attributed to the coaxial cables and connectors, the effect of the wire bonds is most likely the largest contributor. The simulation model likely underestimates or neglects significant parasitic effects in the module and coaxial connections that reduce the effective bandwidth of the assembly.

In order to improve the performance, effort should be put into reducing the effect of the inductive wire bonds, for example by reducing their length, or by using ribbon wire bonds. In addition, by using PD carriers with on-chip 50 Ω terminations near the photodiode output, the effect of signal reflection at the carrier-PCB interface can be reduced. However, this

would also reduce the output current by half, a critical feature of the device.

Successful operation of the JAWS chip depends on the critical current (I_c) of Josephson junctions, which is a parameter that can be tuned in the fabrication process. The peak current of the input pulses should be higher than I_c in order to successfully drive the Josephson arrays [13]. The peak currents demonstrated here are likely sufficient to drive Josephson junction arrays with I_c lower than 3 mA. By increasing the optical power from the laser source, higher peak currents can be achieved.

The ringing will reduce the operation margins in pulse-mode when connected to a JAWS chip. The quantitative evaluation of this reduction will be done by connecting this optical pulse-drive chip to a JAWS circuit in a next step (not described in this paper).

The future final layout will integrate the JAWS array and the PD-multi-chip module on the same chip, which will make obsolete the wire bonds. According to the simulations presented in section II, this will increase the peak currents and reduce ringing significantly. The low profile of the assemblies makes it possible to operate multiple JAWS chips in parallel in the cryoprobe.

ACKNOWLEDGMENT

This work was supported by the EU within the EMPIR JRPs QuADC. The EMPIR is jointly funded in part by the EMPIR participating countries within EURAMET and in part by the European Union. TF received funding from the Academy of Finland (grants 296476 and 306844). The work is part of the Academy of Finland Flagship Programme, Photonics Research and Innovation (PREIN), decision 320168. The authors would like to thank for technical assistance in fabrication of Si carrier chips and PCB assembling Th. Weimann, J. Felgner, K. Stoerr, S. Gruber, and for assistance with wire bonding, Thai Anh Tuan Nguyen.

REFERENCES

[1] S. P. Benz *et al.*, "One-Volt Josephson Arbitrary Waveform Synthesizer," (in English), *Ieee T Appl Supercon,* vol. 25, no. 1, Feb 2015.

[2] O. F. Kieler, R. Behr, R. Wendisch, S. Bauer, L. Palafox, and J. Kohlmann, "Towards a 1 V Josephson Arbitrary Waveform Synthesizer," *Ieee T Appl Supercon,* vol. 25, no. 3, pp. 1-5, 2015.

[3] N. E. Flowers-Jacobs, A. E. Fox, P. D. Dresselhaus, R. E. Schwall, and S. P. Benz, "Two-Volt Josephson Arbitrary Waveform Synthesizer Using Wilkinson Dividers," (in English), *Ieee T Appl Supercon,* vol. 26, no. 6, Sep 2016.

[4] N. E. Flowers-Jacobs *et al.*, "Three volt pulse-driven josephson arbitrary waveform synthesizer," in *2018 Conference on Precision Electromagnetic Measurements (CPEM 2018)*, 2018: IEEE, pp. 1-2.

[5] E. Bardalen, B. Karlsen, H. Malmbekk, O. Kieler, M. N. Akram, and P. Ohlckers, "Packaging, and Demonstration of Optical-Fiber-Coupled Photodiode Array for Operation at 4 K," *IEEE Transactions on Components, Packaging and Manufacturing Technology,* vol. PP, no. 99, pp. 1-7, 2017.

[6] E. Bardalen, B. Karlsen, H. Malmbekk, M. N. Akram, and P. Ohlckers, "Reliability study of fiber-coupled photodiode module for operation at 4 K," *Microelectron Reliab,* 2017.

[7] E. Bardalen, B. Karlsen, H. Malmbekk, M. N. Akram, and P. Ohlckers, "Evaluation of InGaAs/InP photodiode for high-speed operation at 4 K," *International Journal of Metrology and Quality Engineering,* vol. 9, p. 13, 2018.

[8] B. Karlsen *et al.*, "Pulsation of InGaAs photodiodes in liquid helium for driving Josephson arrays in ac voltage realization," *Ieee T Appl Supercon,* vol. 29, no. 7, pp. 1-8, 2019.

[9] O. Kieler *et al.*, "Optical pulse-drive for the pulse-driven AC Josephson voltage standard," *Ieee T Appl Supercon,* vol. 29, no. 5, pp. 1-5, 2019.

[10] E. B. B. Karlsen, J. Nissilä, O. Kieler, L. Palafox, R. Behr, H. Malmbekk, M. N. Akram, and P. Ohlckers, "High-Speed Pulsation of a Cryogenically Operable Bipolar Photodiode Module for the Josephson Arbitrary Waveform Synthesizer," *Conf. Digest CPEM2020,* 2020.

[11] M. Edwards, "The index of refraction of liquid helium," *Canadian Journal of Physics,* vol. 34, no. 8, pp. 898-900, 1956.

[12] J. Nissilä, T. Fordell, O. Kieler, and R. Behr, "Driving a Josephson junction array with a mode-locked laser and a photodiode," in *2018 Conference on Precision Electromagnetic Measurements (CPEM 2018)*, 2018: IEEE, pp. 1-2.

[13] J. M. Williams *et al.*, "The simulation and measurement of the response of Josephson junctions to optoelectronically generated short pulses," *Supercond Sci Tech,* vol. 17, no. 6, pp. 815-818, Jun 2004.